

# Nonequilibrium Currents in Stochastic Field Theories: a Geometric Insight

J. O’Byrne<sup>1</sup>

<sup>1</sup>Université de Paris, Laboratoire Matière et Systèmes Complexes (MSC), UMR 7057 CNRS, F-75205 Paris, France

(Dated: September 30, 2022)

We introduce a new formalism to study nonequilibrium steady-state currents in stochastic field theories. We show that generalizing the exterior derivative to functional spaces allows identifying the subspaces in which the system undergoes local rotations. In turn, this allows predicting the counterparts in the real, physical space of these abstract probability currents. The results are presented for the case of the Active Model B undergoing motility-induced phase separation, which is known to be out of equilibrium but whose steady-state currents have not yet been observed, as well as for the KPZ equation. We locate and measure these currents and show that they manifest in real space as propagating modes localized in regions with non-vanishing gradients of the fields.

Statistical physics aims at describing large-scale phenomena emerging from interacting elementary constituents, ranging from chemicals to animals, from bacteria to traders. Except when systems satisfy detailed balance, no general theory can be systematically applied to study such systems. To understand how microscopic mechanisms drive a system out of equilibrium, physicists have been quantifying the distance to equilibrium using diverse observables, such as the entropy production [1–5], violations of the fluctuation-dissipation theorem [6, 7], or ratchet currents [8–11]. Among those, the stationary probability current plays an important role since its knowledge, together with the stationary probability measure, entirely determine the equations of motion [12–15]. For systems driven out-of-equilibrium by external fields [16–18] or boundary conditions [19, 20], probability currents directly lead to real-space currents—e.g. of energy or mass—that can be observed and quantified easily. In many other situations, as in active systems [21–26], surface growth problems [27] or reaction-diffusion processes [28], probability currents live in high-dimensional configuration spaces and have no simple low-dimensional projection in real space, which makes their study challenging.

While probability currents are well understood for finite-dimensional systems [29–39], collective behaviors are best described at a macroscopic scale using field theory [40–42]. The nonequilibrium nature of such infinite-dimensional description has attracted a lot of interest recently [16, 22, 43–45] but the identification of their *probability* currents remains elusive. Progress has been made in specific situations [46, 47], but a generic framework is crucially lacking.

In this Letter we address this challenge by introducing a new mathematical framework that enables a systematic characterization of steady-state probability currents in nonequilibrium stochastic field theories. This framework is based on a generalization of the curl operator to functional spaces in the form of a functional exterior derivative and on the identification of the appropriate Riemannian metric on the space of fields. We note that a related object, called ‘vertical derivative’, has been introduced for jet bundles [48], a context more restrictive than what we present here. In addition, differential geometry has been formally extended to abstract mathematical spaces [49] but the corresponding level of abstrac-

tion makes such theory hardly applicable to concrete physics problems [15]. Furthermore, these mathematical formalisms have never been applied to characterize probability currents in stochastic field theories. Below, we briefly recap the finite-dimensional case to highlight the key steps of its generalization to infinite dimension. We then detail the construction of the functional exterior derivative for two important examples: the Active Model B (AMB) [50] and the Kardar-Parisi-Zhang (KPZ) equation [27]. Importantly, when undergoing motility-induced phase separation (MIPS), AMB leads to a finite entropy production rate localized at the liquid-gas interface [22, 51]. However, the corresponding probability currents have remained out of reach so far. Here, we show how these currents can be decomposed into superpositions of local 2D rotations, allowing for direct observation (see Fig. 1). Our framework also reveals the direct manifestations of these high-dimensional currents in real space, in the form of propagating modes localized at the liquid-gas interface (see Fig. 2). Similarly, for the KPZ equation, we show how fluctuations are advected along height gradients (see Fig. 4).

To set the stage for stochastic field theories, we start with a quick reminder of the well-known finite-dimensional case. Consider the  $n$ -dimensional Langevin dynamics

$$\dot{\mathbf{r}}(t) = \mathbf{F}(\mathbf{r}(t)) + \sqrt{2D}\boldsymbol{\eta}(t), \quad (1)$$

where  $\mathbf{r}(t) \in \mathbb{R}^n$ ,  $\boldsymbol{\eta}$  is a Gaussian white noise of zero mean and unit variance,  $D$  is the diffusion constant, the mobility has been set to 1, and  $\mathbf{F}$  is an arbitrary smooth vector field. The corresponding Fokker-Planck equation reads  $\partial_t p = -\nabla \cdot \mathbf{J}$ , with  $\mathbf{J} = p\mathbf{F} - D\nabla p$ . In the steady state, the probability current  $\mathbf{J}_s$  encodes the advection of the probability  $p_s$  by the velocity field  $\mathbf{v}_s \equiv \mathbf{J}_s/p_s = \mathbf{F} - D\nabla \log p_s$ . The flow lines of  $\mathbf{v}_s$  indicate the typical trajectories of the system in the steady state [14]. Because it favors certain trajectories over their time-reversed counterparts, the swirling behavior of  $\mathbf{v}_s$  is responsible for the irreversibility of dynamics (1). When  $n = 3$ , it is characterized by the vorticity  $\boldsymbol{\omega}(\mathbf{r}) \equiv \nabla \times \mathbf{v}_s(\mathbf{r}) = \nabla \times \mathbf{F}(\mathbf{r})$  whose norm gives the angular speed of the local swirls, and whose direction is orthogonal to the local 2-dimensional planes in which the current undergoes local rotations. Further, note that the entropy production rate of dynamics (1) is given by  $\sigma = D^{-1} \int \mathbf{J}_s \cdot \mathbf{F} \, d\mathbf{r}$  [5]. Since  $\mathbf{J}_s$

is divergence free and  $\mathbb{R}^n$  simply connected, there is a vector field  $\mathbf{C}$  such that  $\mathbf{J}_s = \nabla \times \mathbf{C}$ . Integrating by parts, one gets  $\sigma = D^{-1} \int \mathbf{C}(\mathbf{r}) \cdot \boldsymbol{\omega}(\mathbf{r}) d\mathbf{r}$ . Hence,  $\boldsymbol{\omega}(\mathbf{r})$  can be seen as the local source of entropy production and  $\mathbf{C}(\mathbf{r})$  as a weight over the infinitesimal loops around  $\mathbf{r}$ .

The generalization to arbitrary finite dimension  $n$  amounts to replacing  $\nabla \times \mathbf{F}$  by  $d\mathbf{F}^b$  in the vorticity  $\boldsymbol{\omega}$ , where  $d$  is the exterior derivative and  $\mathbf{F}^b$  the one-form associated to  $\mathbf{F}$  through a Riemannian metric  $g$  [52]. Denote by  $(\mathbf{e}_i)_{i=1,\dots,d}$  a local basis and  $(dx^i)_{i=1,\dots,d}$  its dual, which satisfies  $dx^i(\mathbf{e}_j) = \delta_j^i$ . Then, to  $\mathbf{F} = \sum_i F^i \mathbf{e}_i$ , we associate the one-form  $\mathbf{F}^b = \sum_i F_i dx^i = \sum_{i,j} g_{ij} F^j dx^i$  with  $g_{ij} \equiv g(\mathbf{e}_i, \mathbf{e}_j)$ . The exterior derivative of  $\mathbf{F}^b$  is then the two-form  $d\mathbf{F}^b$  whose action on arbitrary pairs  $\mathbf{u}, \mathbf{v}$  of vector fields reads

$$d\mathbf{F}^b(\mathbf{u}, \mathbf{v}) = \sum_{i,j=1}^n \left( \frac{\partial F_j}{\partial x_i} - \frac{\partial F_i}{\partial x_j} \right) u^i v^j. \quad (2)$$

Denoting by  $dx^i \wedge dx^j$  the bilinear maps such that  $dx^i \wedge dx^j(\mathbf{u}, \mathbf{v}) = u^i v^j - u^j v^i$ , the vorticity reads

$$\boldsymbol{\omega} \equiv d\mathbf{F}^b = \sum_{1 \leq i < j \leq n} \left( \frac{\partial F_j}{\partial x_i} - \frac{\partial F_i}{\partial x_j} \right) dx^i \wedge dx^j. \quad (3)$$

The prefactor of  $dx^i \wedge dx^j$  in Eq. (3) measures the local rotation induced by  $\mathbf{F}$  in the  $(\mathbf{e}_i, \mathbf{e}_j)$  plane: its sign gives the direction of the rotation and its amplitude the angular speed. Finally, note that dynamics (1) is reversible if and only if  $d\mathbf{F}^b = 0$ . Then,  $\mathbf{F}$  is a gradient and Eq. (1) is a stochastic gradient descent.

We now turn to the core results of this Letter: the generalization of Eq. (3) to infinite-dimensional stochastic field theory and the physical insight it provides on the corresponding systems. For an arbitrary field theory, this requires generalizing the  $b$  and  $d$  operators. The former amounts to finding the Riemannian metric that identifies a reversible dynamics with a gradient descent of the free-energy; it also associates a one form to the deterministic drift. The exterior derivative then extracts the skew-symmetric part of the corresponding Jacobian, which vanishes for equilibrium dynamics and identifies the non-equilibrium circulations otherwise. In this Letter, for sake of clarity, we present these ideas on two important examples, AMB and the KPZ equation. Details of the underlying construction are provided in [15].

*Active Model B.* We start with the study of AMB, which has attracted a lot of interest recently [22, 50], and whose probability currents have remained elusive so far. AMB describes a scalar field whose dynamics is given by

$$\partial_t \rho = -\nabla \cdot \mathbf{j}, \quad \text{where } \mathbf{j} = -\nabla \mu + \sqrt{2D} \boldsymbol{\Lambda}, \quad (4)$$

where  $\boldsymbol{\Lambda}(\mathbf{r}, t)$  is a centered Gaussian white noise field of unit variance and  $\mu$  a nonequilibrium chemical potential defined by

$$\mu([\rho], \mathbf{r}) = a\rho + b\rho^3 - \kappa(\rho)\Delta\rho + \lambda(\rho)|\nabla\rho|^2. \quad (5)$$

Note that  $a, b$  and  $D$  are constants but  $\lambda$  and  $\kappa$  depend on  $\rho(\mathbf{r})$ .

To carry out the aforementioned geometric program, as detailed in [15], we first introduce the space of vector fields  $\boldsymbol{\mu}(\mathbf{r}, [\rho])$  generated by all chemical potentials  $\mu(\mathbf{r}, [\rho])$  through

$$\boldsymbol{\mu}(\mathbf{r}, [\rho]) \equiv -\Delta\mu(\mathbf{r}, [\rho]). \quad (6)$$

This allows rewriting Eq. (4) as  $\partial_t \rho = -\boldsymbol{\mu} + \nabla \cdot \sqrt{2D} \boldsymbol{\Lambda}$  and we now turn to construct the vorticity of  $-\boldsymbol{\mu}$ . Following Otto [53], we define the Riemannian metric

$$g_\rho(\boldsymbol{\mu}_1, \boldsymbol{\mu}_2) \equiv \int \nabla\boldsymbol{\mu}_1(\mathbf{r}, [\rho]) \cdot \nabla\boldsymbol{\mu}_2(\mathbf{r}, [\rho]) d\mathbf{r}. \quad (7)$$

As in finite dimension, this allows associating to any vector field  $\boldsymbol{\mu}_1$  a functional one-form,  $\boldsymbol{\mu}_1^b$ , through  $\boldsymbol{\mu}_1^b(\boldsymbol{\mu}_2) \equiv g(\boldsymbol{\mu}_1, \boldsymbol{\mu}_2)$ . An integration by parts in Eq. (7) gives

$$\boldsymbol{\mu}_1^b(\boldsymbol{\mu}_2) = \int \boldsymbol{\mu}_1(\mathbf{r}, [\rho]) \boldsymbol{\mu}_2(\mathbf{r}, [\rho]) d\mathbf{r}. \quad (8)$$

By analogy with the finite-dimensional case (2), we define the functional exterior derivative of any one-form  $\boldsymbol{\mu}^b$  through its action on an arbitrary pair  $\boldsymbol{\phi}, \boldsymbol{\psi}$  of vector fields:

$$d\boldsymbol{\mu}^b(\boldsymbol{\phi}, \boldsymbol{\psi}) = \int \left[ \frac{\delta\boldsymbol{\mu}(\mathbf{r}, [\rho])}{\delta\rho(\mathbf{r}')} - \frac{\delta\boldsymbol{\mu}(\mathbf{r}', [\rho])}{\delta\rho(\mathbf{r})} \right] \boldsymbol{\phi}(\mathbf{r}') \boldsymbol{\psi}(\mathbf{r}) d\mathbf{r} d\mathbf{r}'. \quad (9)$$

For the chemical potential (5), integrating by parts and rearranging the terms leads to:

$$d\boldsymbol{\mu}^b(\boldsymbol{\phi}, \boldsymbol{\psi}) = \int (2\lambda + \kappa') \nabla\rho \cdot (\boldsymbol{\psi} \nabla\boldsymbol{\phi} - \boldsymbol{\phi} \nabla\boldsymbol{\psi}) d\mathbf{r} \quad (10)$$

where  $\kappa'(\rho) \equiv \frac{d\kappa(\rho)}{d\rho}$ . Finally,  $d\boldsymbol{\mu}^b$  can be rewritten as

$$d\boldsymbol{\mu}^b = \int d\mathbf{r} (2\lambda + \kappa') \nabla\rho \cdot \delta_{\mathbf{r}} \wedge \nabla\delta_{\mathbf{r}}, \quad (11)$$

where  $\delta_{\mathbf{r}}$  is the Dirac delta at position  $\mathbf{r}$  and  $\wedge$  the extension of the finite-dimensional wedge product to distributions such that  $\delta_{\mathbf{r}} \wedge \nabla\delta_{\mathbf{r}}(\boldsymbol{\phi}, \boldsymbol{\psi}) \equiv \boldsymbol{\psi}(\mathbf{r}) \nabla\boldsymbol{\phi}(\mathbf{r}) - \boldsymbol{\phi}(\mathbf{r}) \nabla\boldsymbol{\psi}(\mathbf{r})$ .

The vorticity  $\boldsymbol{\omega}$  of the deterministic drift of Eq. (4) is then given by  $\boldsymbol{\omega} \equiv -d\boldsymbol{\mu}^b$ . Equation (9) shows that  $\boldsymbol{\omega} = 0$  corresponds to the Schwarz condition for  $\mu$  to be the functional derivative of a free energy [54, 55]. For AMB, this amounts to  $2\lambda + \kappa' = 0$  [50, 56].

Comparing Eq. (11) to Eq. (3), the discrete sum over  $dx_i \wedge dx_j$  has been replaced by an integral over  $\delta_{\mathbf{r}} \wedge \nabla\delta_{\mathbf{r}}$ . Equation (11) can thus be interpreted as follows: the flow lines of  $-\boldsymbol{\mu}$  swirl around a given point  $\rho$  in  $\mathbb{F}$  as soon as  $(2\lambda + \kappa') \nabla\rho \neq 0$ . As in the finite-dimensional setting, such a local swirl corresponds to an infinitesimal rotation that can be decomposed into the superposition of rotations occurring in the spaces  $(\rho(\mathbf{r}), \partial_x \rho(\mathbf{r}), \partial_y \rho(\mathbf{r}))$  wherever  $(2\lambda + \kappa') \nabla\rho(\mathbf{r}) \neq 0$ . All in all, the flow lines of the deterministic drift tend to rotate in the 2D plane  $(\rho(\mathbf{r}), \partial_k \rho(\mathbf{r}))$ :

$$\begin{cases} \text{counter-clockwise} & \text{iff } [2\lambda + \kappa'] \partial_k \rho(\mathbf{r}) > 0 \\ \text{clockwise} & \text{iff } [2\lambda + \kappa'] \partial_k \rho(\mathbf{r}) < 0 \end{cases} \quad (12)$$

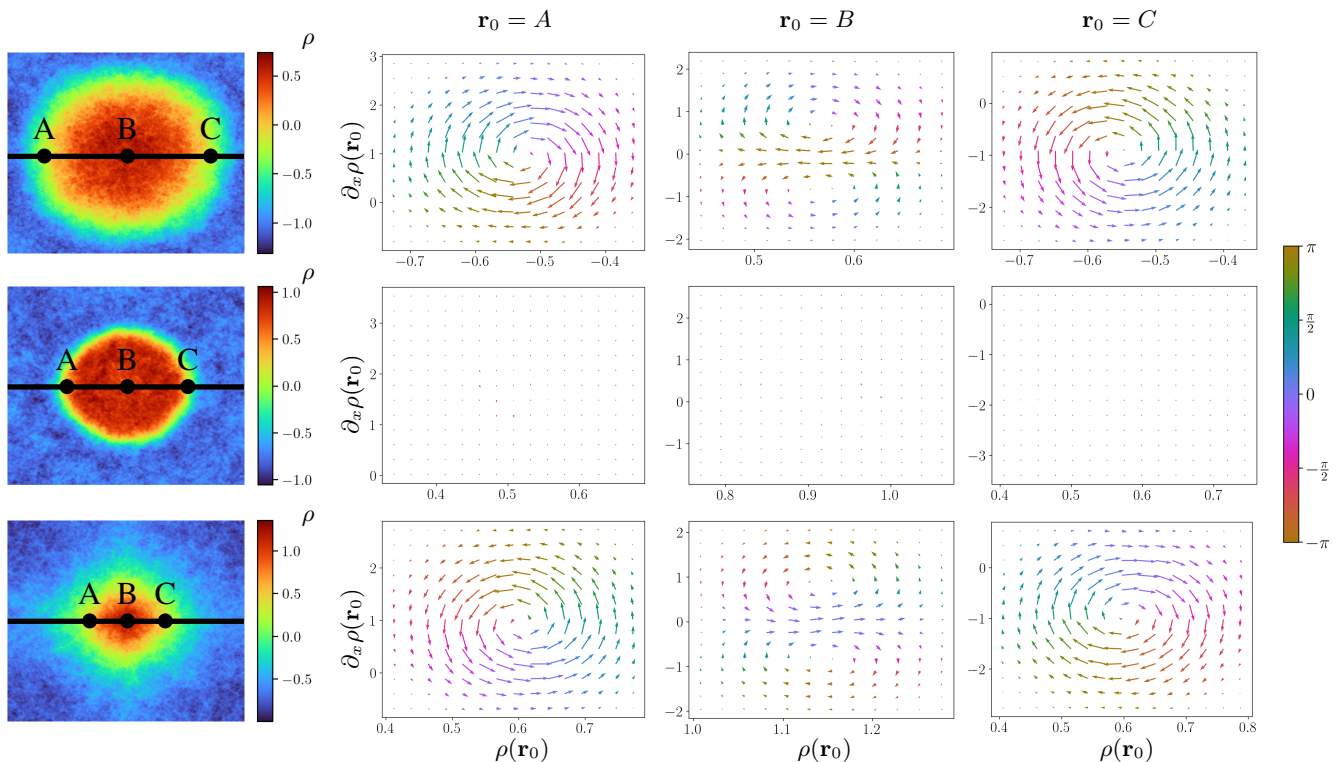


FIG. 1. Measurements of the stationary probability currents in the planes  $(\rho(\mathbf{r}_0), \partial_x \rho(\mathbf{r}_0))$  at representative points in phase-separated systems, using numerical resolution of Eq. (4). The rows corresponds to  $2\lambda + \kappa' < 0$  (top),  $2\lambda + \kappa' = 0$  (center), and  $2\lambda + \kappa' > 0$  (bottom), respectively. The average stationary profiles are shown in the left column. Other columns show the current vector fields measured at the corresponding points  $\mathbf{r}_0 = A, B, C$  in the phase-separated profiles. (Arrow colors encode their angles with respect to  $\mathbf{e}_x$ .) Parameters:  $a = -1$ ,  $b = 1$ ,  $\kappa = 0.1$ , average density  $\rho_0 = -0.4$ ,  $D = 10^{-3}$ ,  $L_x = L_y = 10$  and  $\lambda = -2$  (top), 0 (center) and 2 (bottom). See [15] for numerical details.

at speed given by the amplitude of  $(2\lambda + \kappa')\partial_k \rho(\mathbf{r})$ .

Let us now show that these predictions allow measuring the steady-state currents of a phase-separated AMB. We denote by  $\rho_s(\mathbf{r}) \equiv \langle \rho(\mathbf{r}) \rangle$  the stationary average profile of the fluctuating field  $\rho$ . We then measure the probability current in the plane  $(\rho(\mathbf{r}), \partial_x \rho(\mathbf{r}))$  at three different positions (points A, B and C - see Fig. 1) along the horizontal diameter of the liquid droplet. As predicted, changing the sign of  $2\lambda + \kappa'$  (top vs. bottom row of Fig. 1) or that of  $\partial_x \rho$  (column A vs. C) changes the direction of the circulation. Furthermore, the probability current vanishes in the equilibrium case  $2\lambda + \kappa' = 0$  (center row), as expected.

Note that, at the interface,  $\rho(\mathbf{r}) \simeq \rho_s(\mathbf{r})$  and  $\nabla \rho(\mathbf{r}) \simeq \nabla \rho_s(\mathbf{r})$  so that  $\mathfrak{d}\mu^b|_{\rho} \simeq \mathfrak{d}\mu^b|_{\rho_s}$ , which corresponds to uniform rotations in each space  $(\rho(\mathbf{r}), \nabla \rho(\mathbf{r}))$ . The latter give rise to the leading order terms of the current in the noise amplitude (columns A and C). On the contrary, in the bulk,  $\nabla \rho(\mathbf{r}) \simeq \nabla \delta \rho(\mathbf{r})$ , where  $\delta \rho \equiv \rho - \rho_s$ . This leads to weaker, higher order currents (column B).

It is tempting to split the chemical potential into  $\mu = \mu_{\text{eq}} + \mu_{\text{act}}$ , where  $\mu_{\text{eq}}$  is the functional derivative of a free energy  $\mathcal{F}$  whereas  $\mu_{\text{act}}$  is not integrable, so as to identify  $\mu_{\text{act}}$  as the source of irreversibility. Unfortunately, such a decomposi-

tion is not unique, since adding a functional derivative  $\delta \mathcal{G} / \delta \rho$  to  $\mu_{\text{eq}}$  and subtracting it from  $\mu_{\text{act}}$  yields another equivalent decomposition. On the contrary,  $\mathfrak{d}\mu^b$  can unambiguously be identified as the source of irreversibility since the set of functional derivatives exactly coincides with the kernel of  $\mathfrak{d}$ , so that

$$\mathfrak{d}\mu^b = \mathfrak{d}\mu_{\text{act}}^b = \mathfrak{d}(\mu_{\text{act}}^b + \delta \mathcal{G} / \delta \rho). \quad (13)$$

*Propagating modes.* Let us now show how our formalism yields a valuable insight into the dynamics of fluctuations. In Fig. 2a-c, we show the short-time relaxations of a perturbation  $\delta \rho = \varepsilon \cos(qx)$  around a phase-separated profile  $\rho_s$  for  $2\lambda + \kappa'$  negative, null or positive. To best compare the three cases, we use the same  $\rho_s$ , corresponding to a stationary droplet for  $2\lambda + \kappa' = 0$  (see Fig. 2d). The analysis, detailed in Fig. 3, of the current constructed in Fig. 1 predicts that the perturbation propagates at the interface, from the liquid to the gas when  $2\lambda + \kappa' < 0$  and vice versa if  $2\lambda + \kappa' > 0$ . In the equilibrium case, on the contrary, the perturbation is predicted to relax to  $\delta \rho = 0$  while remaining stationary. These predictions are confirmed by the simulations shown in Figs. 2a-c.

Figure 2 shows the advection of initial perturbations by the deterministic drift. In the presence of a finite noise, superpositions of the corresponding propagating modes will be

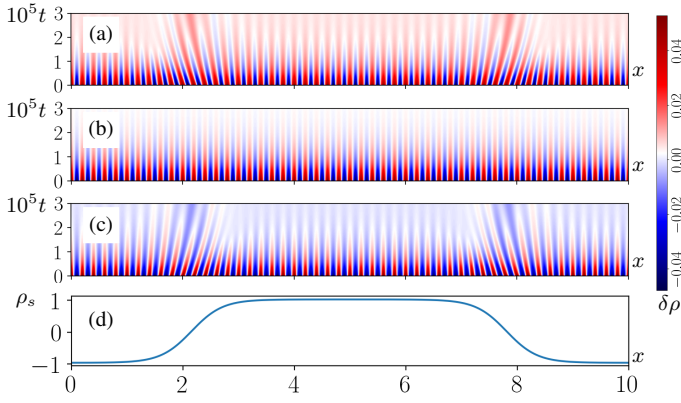


FIG. 2. Evolution of a perturbation  $\delta\rho$  around the equilibrium profile  $\rho_s$  under the AMB dynamics (4) using periodic boundary conditions and  $\delta\rho(x, y, t = 0) = \varepsilon \cos(100\pi x/L_x)$ . Panels (a-c) are kymographs representing the evolution of  $\delta\rho(x, L_y/2, t)$ . Panel (d) is a cut of  $\rho_s$  at  $y = L_y/2$ . Parameters:  $\rho_0 = -0.45$ ,  $a = -1$ ,  $b = 1$ ,  $\kappa = 0.15$ ,  $dt = 10^{-7}$ ,  $dx = dy = 10^{-2}$ ,  $L_x = L_y = 10$ ,  $\varepsilon = 0.05$ , and  $\lambda = -4, 0$  and  $4$  for panels (a), (b) and (c), respectively. Time axis unit of the kymographs is  $\Delta t = 10^{-5}$ .

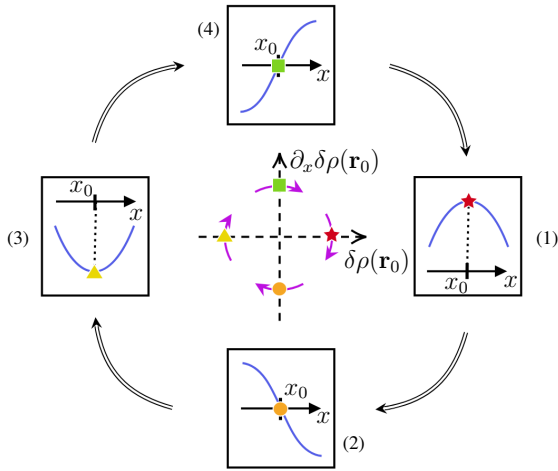


FIG. 3. Analysis of the currents shown in Fig. 1 predicting the mode propagation reported in Fig. 2. Consider the case  $2\lambda + \kappa' < 0$  and a point  $\mathbf{r}_0 = (x_0, L_y/2)$  on the left boundary of the droplet (top row, column A of Fig. 1). In the central panel above, we show the circulation induced by the current in the  $(\delta\rho(\mathbf{r}_0), \partial_x \delta\rho(\mathbf{r}_0))$  plane. Consider a perturbation such that  $\delta\rho(\mathbf{r}_0)$  is a local maximum at  $t = 0$  (panel (1), red star). As time goes on, the current drives the fluctuation sequentially from (1) to (2) (orange dot), to (3) (yellow triangle), to (4) (green square). Each panel shows the fluctuation profile  $\delta\rho(x, L_y/2)$  around  $x_0$  (blue curves). These successive states of  $\delta\rho$  shows that the probability current corresponds to a leftward propagation of  $\delta\rho$  in the real space, from the liquid to the gas phase. Inspection of Fig. 1 allows predicting all the dynamics reported in Fig. 2.

constantly excited. Hence, to leader order in the noise, density fluctuations propagate radially at the interface, outwards or inwards, depending on the sign of  $2\lambda + \kappa'$ . This is the main real-space manifestation of the steady-state probability current. It suggests a natural mechanism to account for the continuous expulsion of bubbles, from the bubbly liquid to the gas phase, observed in the active model B + [57]. We note that higher order contributions will also include orthoradial fluctuations. The latter are particularly interesting since their dynamics could offer insight on surface tension effects or capillary waves, which have recently attracted a lot of interest [58–66].

*KPZ equation.* Consider the celebrated KPZ equation [27]

$$\partial_t h = -\mu + \sqrt{2D}\Lambda, \quad \mu(\mathbf{r}, [h]) = \lambda|\nabla h|^2 - \kappa\Delta h. \quad (14)$$

Here,  $-\mu$  can be directly considered a vector field on  $\mathbb{F}$  and the appropriate Riemannian metric to construct the vorticity is the usual  $L^2$ -scalar product [15]:

$$g_h(\mu_1, \mu_2) = \int \mu_1(\mathbf{r}, [h])\mu_2(\mathbf{r}, [h]) d\mathbf{r}. \quad (15)$$

In this geometry, the one-form  $\mu^\flat(\cdot) \equiv g(\mu, \cdot)$  associated to a vector field  $\mu(\mathbf{r}, [h])$  again corresponds to integration against  $\mu$ , and the vorticity of the deterministic drift of Eq. (14) is again  $\omega = -\text{d}\mu^\flat$  where  $\text{d}\mu^\flat = \int d\mathbf{r}(2\lambda + \kappa')\nabla h \cdot \delta_{\mathbf{r}} \wedge \nabla \delta_{\mathbf{r}}$ . The analysis conducted above for AMB can then be directly transposed to KPZ. We thus predict that fluctuations around a height profile  $h$  should again propagates upward or downward  $\nabla h$ , depending on the sign of  $2\lambda + \kappa'$ . These predictions are confirmed by the simulations shown in Fig. 4.

We stress that the KPZ equation and AMB describe fundamentally different physics: the unbounded growth of a fluctuating interface and the nonequilibrium phase separation of a conserved field leading to a well defined stationary profile. These distinct long-term behaviors stem from the different irrotational component of their determinist drifts. Importantly, our analysis reveal that, on the contrary, these systems share

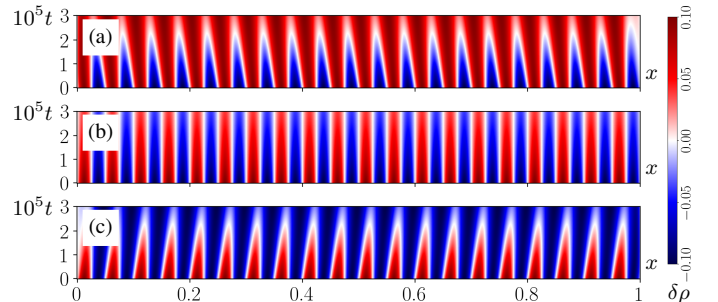


FIG. 4. Kymographs showing the zero-noise relaxation of a perturbation  $\delta h(x) = 0.1 \sin(40\pi x)$ , added at time  $t = 0$  to a linear profile  $h(x) = 10x$ , under the KPZ dynamics (14) with Dirichlet boundary conditions. Parameters:  $\nu = 2$  and  $\lambda = -16, 0, 16$  for panels (a), (b) and (c), respectively. System size  $L = 1$ . Space and time discretization:  $dx = 10^{-3}$  and  $dt = 10^{-7}$ .

the same vorticity. In turn, this leads to an unexpected similarity in the dynamics of fluctuations, as seen by comparing Figs. 2&4.

*Discussion.* In this Letter, we introduced a new formalism to characterize the infinite-dimensional probability currents of (stochastic) field theories without requiring the knowledge of their stationary probability. This allowed us to determine their low-dimensional measurable projections as well as to predict their manifestations in the real, physical space. Our formalism is based based on the generalization to functional spaces of the exterior derivative. The latter offers a new, local and unambiguous criterion to characterize the departure from equilibrium of coarse-grained systems.

While we have focused here on AMB and the KPZ equation, both for sake of clarity and due to the interest they have attracted over the years, we note that our theoretical framework can be generalized to any overdamped fluctuating hydrodynamics with Gaussian noise. Suppose for instance that the chemical potential of Eq. (4) or (14) is given by a fourth order expansion in gradient of  $\rho$ , i.e.  $\mu = \mu_0 + \lambda|\nabla\rho|^2 - \kappa\Delta\rho + \alpha_1\Delta^2\rho + \alpha_2|\nabla\rho|^4 + \alpha_3|\nabla\rho|^2\Delta\rho + \alpha_4(\Delta\rho)^2 + \alpha_5\nabla\rho\cdot\nabla\Delta\rho$ , where  $\mu_0$  is a local function of  $\rho$  and where, for the sake of clarity, all the other coefficients are taken to be constant. This situation leads to  $d\mu^b = \int dr ([2\lambda\nabla\rho + 4\alpha_2|\nabla\rho|^2\nabla\rho + (\alpha_5 - 2\alpha_4)\nabla\Delta\rho]\cdot\delta_r \wedge \nabla\delta_r + \alpha_5\nabla\rho\cdot\delta_r \wedge \nabla\Delta\delta_r)$ . Our framework thus predicts the probability currents to be localized in the spaces  $(\rho(\mathbf{r}), \nabla\rho(\mathbf{r}))$  and  $(\rho(\mathbf{r}), \nabla\Delta\rho(\mathbf{r}))$ . More generally, generalizing our framework to non-local interactions, vector or tensor fields, as well as for active mixtures [67–69] is an exciting program for the future.

*Acknowledgments.* The author thanks Yariv Kafri, Julien Tailleur and Frédéric van Wijland for useful comments on the manuscript.

- 
- [1] J. L. Lebowitz and H. Spohn, *Journal of Statistical Physics* **95**, 333 (1999).
- [2] J. Kurchan, *Journal of Physics A: Mathematical and General* **31**, 3719 (1998).
- [3] C. Maes, *Journal of statistical physics* **95**, 367 (1999).
- [4] T. Hatano and S.-i. Sasa, *Physical review letters* **86**, 3463 (2001).
- [5] U. Seifert, *Physical review letters* **95**, 040602 (2005).
- [6] L. F. Cugliandolo, *Journal of Physics A: Mathematical and Theoretical* **44**, 483001 (2011).
- [7] A. Pérez-Madrid, D. Reguera, and J. Rubi, *Physica A: Statistical Mechanics and its Applications* **329**, 357 (2003).
- [8] R. P. Feynman, R. B. Leighton, and M. Sands, *The Feynman lectures on physics, Vol. I: The new millennium edition: mainly mechanics, radiation, and heat*, Vol. 1 (Basic books, 2011).
- [9] J. M. Parrondo and P. Español, *American Journal of Physics* **64**, 1125 (1996).
- [10] P. Hänggi and F. Marchesoni, *Reviews of Modern Physics* **81**, 387 (2009).
- [11] M. O. Magnasco, *Physical Review Letters* **71**, 1477 (1993).
- [12] R. Zia and B. Schmittmann, *Journal of Statistical Mechanics: Theory and Experiment* **2007**, P07012 (2007).
- [13] R. Zia and B. Schmittmann, *Physics Procedia* **7**, 112 (2010).
- [14] T. B. Liverpool, arXiv preprint arXiv:1810.10980 (2018).
- [15] See Supplemental Material [url], which includes theoretical and numerical details.
- [16] L. Bertini, A. De Sole, D. Gabrielli, G. Jona-Lasinio, and C. Landim, *Reviews of Modern Physics* **87**, 593 (2015).
- [17] B. Schmittmann and R. K. Zia, *Phase transitions and critical phenomena* **17**, 3 (1995).
- [18] G. L. Eyink, J. L. Lebowitz, and H. Spohn, *Journal of Statistical physics* **83**, 385 (1996).
- [19] B. Derrida, J. Lebowitz, and E. Speer, *Journal of statistical physics* **107**, 599 (2002).
- [20] T. Bodineau and B. Derrida, *Physical review letters* **92**, 180601 (2004).
- [21] J. Tailleur and M. Cates, *Physical review letters* **100**, 218103 (2008).
- [22] C. Nardini, É. Fodor, E. Tjhung, F. Van Wijland, J. Tailleur, and M. E. Cates, *Physical Review X* **7**, 021007 (2017).
- [23] É. Fodor, C. Nardini, M. E. Cates, J. Tailleur, P. Visco, and F. Van Wijland, *Physical review letters* **117**, 038103 (2016).
- [24] J. O’Byrne, Y. Kafri, J. Tailleur, and F. van Wijland, *Nature Review Physics* **4**, 167 (2022).
- [25] P. Galajda, J. Keymer, P. Chaikin, and R. Austin, *Journal of bacteriology* **189**, 8704 (2007).
- [26] E. Flenner and G. Szamel, *Physical Review E* **102**, 022607 (2020).
- [27] M. Kardar, G. Parisi, and Y.-C. Zhang, *Physical Review Letters* **56**, 889 (1986).
- [28] H. Hinrichsen, *Advances in physics* **49**, 815 (2000).
- [29] M. Baiesi and C. Maes, *New Journal of Physics* **15**, 013004 (2013).
- [30] S. Dal Cengio, D. Levis, and I. Pagonabarraga, *Journal of Statistical Mechanics: Theory and Experiment* **2021**, 043201 (2021).
- [31] H. Ge, *Physical Review E* **89**, 022127 (2014).
- [32] M. Baiesi, E. Boksenbojm, C. Maes, and B. Wynants, *Journal of statistical physics* **139**, 492 (2010).
- [33] N. Freitas, J.-C. Delvenne, and M. Esposito, *Physical Review X* **10**, 031005 (2020).
- [34] J. Kurchan, arXiv preprint arXiv:0901.1271 (2009).
- [35] M. Kaiser, R. L. Jack, and J. Zimmer, *Journal of Statistical Physics* **170**, 1019 (2018).
- [36] X. Fang, K. Kruse, T. Lu, and J. Wang, *Reviews of Modern Physics* **91**, 045004 (2019).
- [37] H. Feng and J. Wang, *The Journal of chemical physics* **135**, 234511 (2011).
- [38] J. Wang, *Advances in Physics* **64**, 1 (2015).
- [39] M. Polettini, *EPL (Europhysics Letters)* **97**, 30003 (2012).
- [40] U. C. Täuber, *Critical dynamics: a field theory approach to equilibrium and non-equilibrium scaling behavior* (Cambridge University Press, 2014).
- [41] M. Kardar, *Statistical physics of fields* (Cambridge University Press, 2007).
- [42] J. Cardy, *Scaling and renormalization in statistical physics*, Vol. 5 (Cambridge university press, 1996).
- [43] Ø. L. Borthne, É. Fodor, and M. E. Cates, *New Journal of Physics* **22**, 123012 (2020).
- [44] F. Caballero and M. E. Cates, *Physical Review Letters* **124**, 240604 (2020).
- [45] Y. I. Li and M. E. Cates, *Journal of Statistical Mechanics: Theory and Experiment* **2021**, 013211 (2021).
- [46] J. Gladrow, N. Fakhri, F. C. MacKintosh, C. Schmidt, and C. Broedersz, *Physical review letters* **116**, 248301 (2016).
- [47] C. Battle, C. P. Broedersz, N. Fakhri, V. F. Geyer, J. Howard,

- C. F. Schmidt, and F. C. MacKintosh, *Science* **352**, 604 (2016).
- [48] I. M. Anderson, *The variational bicomplex*, Tech. Rep. (Utah State Technical Report, 1989, <http://math.usu.edu/fgmp>, 1989).
- [49] A. Kriegl and P. W. Michor, *The convenient setting of global analysis*, Vol. 53 (American Mathematical Soc., 1997).
- [50] R. Wittkowski, A. Tiribocchi, J. Stenhammar, R. J. Allen, D. Marenduzzo, and M. E. Cates, *Nature communications* **5**, 1 (2014).
- [51] D. Martin, J. O’Byrne, M. Cates, É. Fodor, C. Nardini, J. Tailleur, and F. van Wijland, arXiv preprint arXiv:2008.12972.
- [52] D.-Q. Jiang and D. Jiang, *Mathematical theory of nonequilibrium steady states: on the frontier of probability and dynamical systems* (Springer Science & Business Media, 2004).
- [53] F. Otto, *Communications in Partial Differential Equations* **26**, 101 (2001).
- [54] J. O’Byrne and J. Tailleur, *Physical Review Letters* **125**, 208003 (2020).
- [55] T. Grafke, M. E. Cates, and E. Vanden-Eijnden, *Physical review letters* **119**, 188003 (2017).
- [56] A. P. Solon, J. Stenhammar, M. E. Cates, Y. Kafri, and J. Tailleur, *Physical Review E* **97**, 020602 (2018).
- [57] E. Tjhung, C. Nardini, and M. E. Cates, *Physical Review X* **8**, 031080 (2018).
- [58] J. Bialké, J. T. Siebert, H. Löwen, and T. Speck, *Physical review letters* **115**, 098301 (2015).
- [59] U. M. B. Marconi, C. Maggi, and S. Melchionna, *Soft Matter* **12**, 5727 (2016).
- [60] S. Paliwal, V. Prymidis, L. Filion, and M. Dijkstra, *The Journal of chemical physics* **147**, 084902 (2017).
- [61] A. Patch, D. M. Sussman, D. Yllanes, and M. C. Marchetti, *Soft matter* **14**, 7435 (2018).
- [62] R. Wittmann, F. Smallenburg, and J. M. Brader, *The Journal of chemical physics* **150**, 174908 (2019).
- [63] R. Zakine, Y. Zhao, M. Knežević, A. Daerr, Y. Kafri, J. Tailleur, and F. van Wijland, *Physical Review Letters* **124**, 248003 (2020).
- [64] A. Wysocki and H. Rieger, *Physical Review Letters* **124**, 048001 (2020).
- [65] A. K. Omar, Z.-G. Wang, and J. F. Brady, *Physical Review E* **101**, 012604 (2020).
- [66] N. Lauersdorf, T. Kolb, M. Moradi, E. Nazockdast, and D. Klotsa, *Soft Matter* **17**, 6337 (2021).
- [67] S. Saha, J. Agudo-Canalejo, and R. Golestanian, *Physical Review X* **10**, 041009 (2020).
- [68] Z. You, A. Baskaran, and M. C. Marchetti, *Proceedings of the National Academy of Sciences* **117**, 19767 (2020).
- [69] A. Dinelli, J. O’Byrne, A. Curatolo, Y. Zhao, P. Sollich, and J. Tailleur, arXiv preprint arXiv:2203.07757 (2022).